# Internal Wave Breaking Dynamics and Associated Mixing in the Coastal Ocean

**Eiji Masunaga**, Ibaraki University, Hitachi, Japan
**Robert S Arthur**, Lawrence Livermore National Laboratory, Livermore, CA, United States
**Oliver B Fringer**, Stanford University, Stanford, CA, United States





## Introduction

When internal waves interact with shallow slopes in the coastal ocean, they become highly nonlinear and break, accompanied by turbulent mixing. Internal wave breaking processes are similar to those of surface waves breaking on a beach (Fig. 1). However, despite their ubiquity in the coastal ocean, the complex, transient nature of breaking internal wave events makes them difficult to predict and observe. The small spatial and temporal scales associated with breaking internal waves and the resulting stratified turbulence only add to this greater difficulty. Recently developed observational approaches, including high-resolution towed instruments, mooring systems, and autonomous underwater vehicles, have revealed new insights into internal wave breaking processes, while improved laboratory and numerical modeling techniques have also been used to study their dynamics in more detail. In this article, the results of recent observational, laboratory, and numerical modeling studies of internal wave breaking are presented with a focus on turbulent mixing in shallow coastal regions.

## Internal Tide Breaking

Internal tides are internal waves of tidal frequency in the ocean (*see Internal Tides*) and are generated by the interaction of tidal currents with topographic slopes. Thus, continental shelf breaks and oceanic ridges are known as "hot spots" of internal tide generation. Internal tide energy typically radiates away from generation sites in the form of beams that propagate at a shallow angle relative to the horizontal (roughly 1°–3°), bouncing up and down as they reflect from the base of the mixed layer and bottom topography. These beams are composed of a superposition of oscillatory modes of motion ranging in vertical wavelengths from those that are on the order of the depth of the water column (the so-called "low modes") to many fractions of the depth (the so-called "high modes"). Because the high modes tend to dissipate their energy relatively quickly, most of the internal tide energy that radiates far from generation sites is in the form of the first low mode, wherein fluid parcels oscillate predominantly in the horizontal and those at the surface are 180° out of phase with those toward the bottom, with particle motions being small at a node somewhere near 1/3 the depth from the surface. The result is that the first vertical internal wave mode dominates in shallow continental shelf regions far from generation sites. Internal tides can induce large isopycnal displacements, sometimes exceeding 100 m. On continental shelves, the horizontal propagation speed of internal tides is of the order of 0.1–1 m $s^{-1}$ and the wavelength is 10–50 km.

When internal tides propagate onto a shallow slope (with a depth less than the offshore pycnocline/thermocline depth), the wave speed is limited by the shallow bathymetry and the wave steepness increases, resulting in highly nonlinear wave motions. Such nonlinear internal waves propagating on a shallow slope are often referred to as "internal bores" or "internal tidal bores," and give rise to an abrupt change in time of temperature and density, as shown in Figure 2C and D. Internal tides and bores ultimately break on slopes due to their nonlinearity and some of the incoming wave energy is lost to turbulent mixing and dissipation, while the remaining energy is reflected back offshore. The intensity of turbulent mixing due to a breaking internal tide can be 10,000 times larger than the background value.

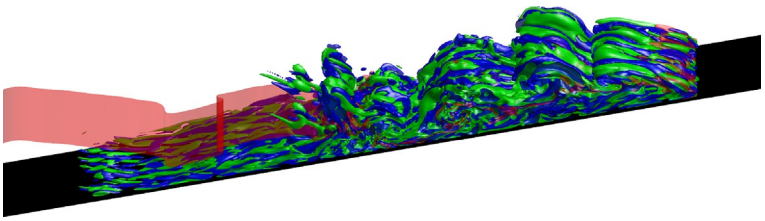

**Fig. 1** A three-dimensional view of an internal wave breaking on a slope from the direct numerical simulations of Arthur et al. (2017). The density interface is shown in *red*, while positive/negative cross-shore vorticity surfaces are shown in *blue*/*green*.

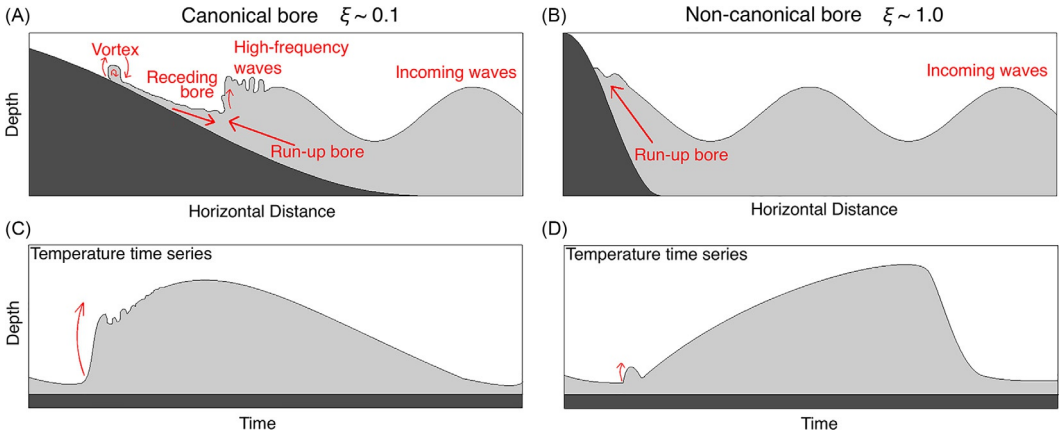


**Fig. 2** Schematics of (A, C) canonical bores and (B, D) noncanonical bores. Upper panels (A, B) show the vertical cross-section of the wave structure and lower panels (C, D) show temperature/density time series on a slope. The *light gray color* indicates denser or colder water.

## Classification of Internal Bores

The intensity of turbulence due to breaking internal waves on slopes depends on a ratio of the topographic slope to the wave steepness, known as the internal Iribarren number

$$\xi = \frac{s}{\sqrt{a/\lambda}}, \tag{1}$$

which is analogous to the Iribarren number for surface wave breaking (see Boegman et al., 2005). Here, $s$ is the topographic slope (that is, $|dD/dx|$, where $D$ is the depth) and $a/\lambda$ is a measure of the wave steepness, where $a$ is a measure of the internal wave amplitude and $\lambda$ is the wavelength. The internal wave steepness is proportional to the internal Froude number ($Fr_i = a/\lambda$), which is a measure of the wave nonlinearity given that it represents a ratio of the internal wave-driven fluid velocity to the internal wave speed. Therefore, internal Froude numbers exceeding unity imply wave overturning because the fluid velocity exceeds the wave speed. The internal Froude number can be expressed in terms of the topographic slope and the Iribarren number with $Fr_i = (s/\xi)^2$, implying that low Iribarren number conditions lead to nonlinear motion and instability because of high internal Froude number conditions.

Generally speaking, the turbulence intensity due to wave breaking increases with decreasing internal Iribarren number. Therefore, nearly all of the incoming internal wave energy is lost to turbulent mixing and dissipation during breaking when the Iribarren number is small, while the turbulence intensity is weak and most of the incoming wave energy reflects offshore when the Iribarren number is large. Based on these ideas, internal bores can be classified into two general categories depending on the internal Iribarren number, namely canonical bores ($\xi \ll 1$) and noncanonical bores ($\xi = \mathrm{O}(1)$), each with distinct dynamics and turbulent mixing qualities.

### *Canonical bores*

Canonical bores occur for gentle slope or steep wave (i.e., low Iribarren number, $\xi \ll 1$) conditions and are classified as such because they are the most frequently observed in coastal oceans. In the case of canonical bores, internal waves shoal gradually over a shallow slope resulting in a steep leading wave front accompanied by a sharp drop in temperature over time, followed by a gradually-varying trailing wave front accompanied by a slow increase in temperature with time (Fig. 2C). Due to the periodic nature of internal tides, internal bores can repeatedly impact a coastal slope. An important feature of canonical bores is thus the interaction of an onshore propagating bore with the receding currents associated with the bore from the previous internal tide. This process is shown in Fig. 2A. An example of the observed temperature structure associated with internal tide breaking is shown in Fig. 3 (Masunaga et al., 2016). The interaction of a bore and the receding current from the previous shoaling internal tide appears

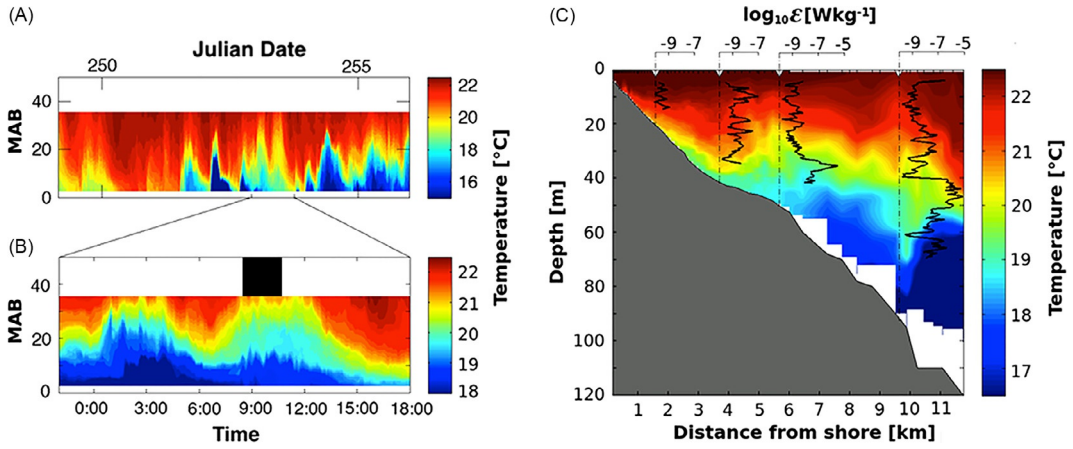


**Fig. 3** Observed internal tide breaking structure in a shallow bay (Otsuchi Bay, Japan) due to a canonical bore from Masunaga et al. (2016). (A, B) Temperature time series, and (C) temperature (color) and rate of turbulent kinetic energy dissipation (*black lines*). The *black shaded area* in panel (B) indicates the period of the transect observation shown in panel (C).

approximately 5 km from shore in Fig. 3C. Observed data from a microstructure profiler shows a strong turbulent mixing event within which the rate of dissipation of turbulent kinetic energy reaches $8 \times 10^{-6}$ W kg$^{-1}$, which is 1000–10,000 times higher than the background value. Numerical simulations and laboratory experiments show that nearly all (roughly 90%) of incoming wave energy is dissipated due to wave breaking for low Iribarren number conditions ($\xi \sim 0.1$).

The breaking event induced by the interaction of receding currents and incident bores enhances mixing not only near the bottom, but over the entire water column. In some cases, canonical bores contribute to mixing of the fresh water associated with near-surface river plumes. In addition, the interaction of a buoyant river plume with internal tidal bores induces shoreward high-frequency nonlinear solitary waves which produce strong mixing at the river mouth (Sasmal et al., 2018).

Once the internal tide that produced the internal bore begins to recede, the internal bore continues to propagate upslope as a vortex core that eventually dissipates in shallower water (Fig. 2A). This vortex core, often referred to as an "internal bolus," causes enhanced near-bottom mixing on the slope over vertical scales associated with the bolus, which are typically several tens of meters in coastal regions. The vorticity in upslope-propagating boluses is enhanced by strong vertical shear resulting from the interaction of the receding flow of the previous internal tide with the strong near-bottom shoreward flow associated with the bore head. This can produce upward currents in the vortex core exceeding 0.1 m s$^{-1}$. Due to the difficulty in observing these relatively small-scale bolus features, numerical models are often used to investigate their dynamics.

### *Noncanonical bores*

Noncanonical bores occur for steep topographic or small wave slope (i.e., high Iribarren number, $\xi \sim 1.0$) conditions, and are not as common in the coastal ocean. Monterey Bay, CA, United States is known as a place where this type of bore frequently occurs due to the steep slope in the inner part of the bay. In contrast to canonical bores, the temperature signal associated with a noncanonical bore shows a gradual decrease in temperature as the bore passes, followed by a rapid increase in temperature as the bore recedes (Figure 2B and D). The near-bottom currents and vertical shear are higher during the relaxation phase (when the bore recedes downslope) than during the run-up phase. Thus, turbulent mixing is enhanced during the relaxation. However, because receding flows do not generally interact with the subsequent bore, wave breaking is weaker and the turbulence intensity is much smaller than it is for canonical wave breaking. Although a vortex core is generated at the head of a noncanonical bore, the intensity of upward flows is typically weak. Roughly half of incoming wave energy is reflected back offshore (and therefore not dissipated) in high Iribarren number conditions, as compared to only 10% for canonical bores.

## Intermittency of Internal Tide Breaking

Internal tide breaking is intermittent and is not always correlated with sea-surface (barotropic) tidal elevations. Although the internal tide is typically generated by the barotropic tide, the motion of an isotherm due to an internal tide is not generally in phase with the barotropic tide, nor does it arrive at intervals associated with the expected tidal period (i.e., every 12.42 h for the semidiurnal internal tide). This discrepancy occurs because (1) internal tides are typically generated far from where they are observed and are therefore not consistent with local tidal elevations and (2) internal tide phase speeds are modulated by stratification, barotropic tidal flows, and other background flows. As a result, the propagation time from the generation site to the observation site can vary from one internal tide to the next.

Furthermore, nonlinear bores can be highly intermittent because they depend on the local position at which the pycnocline intersects the bathymetry. For example, on continental shelves at mid- to high latitudes, the diurnal internal tidal frequency can be lower than the local inertial frequency, producing trapped diurnal internal tides that propagate along continental shelves. These can

drive strong diurnal oscillations in the pycnocline that modulate the nonlinear bores associated with the semidiurnal internal tide that propagates normal to the shelf. Therefore, nonlinear bores can be absent if the pycnocline is moved offshore and away from the observation site depending on the phase of the diurnal internal tide. Similarly, upwelling dynamics in eastern boundary current systems can lead to seasonal oscillations in the pycnocline that may also affect the formation of internal bores.

## Internal Solitary Wave Breaking

Because internal tides typically propagate over long distances prior to breaking, they usually steepen into trains of internal solitary waves before encountering shelf topography where they break. Therefore, internal tide breaking dynamics can often be described in terms of the dynamics of breaking internal solitary waves. While internal tides in the open ocean can have wavelengths exceeding 100 km, steepening leads to much shorter internal waves with wavelengths as small as 100 s of meters in the coastal ocean. The result is internal waves with lower Iribarren numbers (steeper waves for fixed bottom slope) upon breaking.

According to theory, internal solitary waves exist as a balance between nonlinearity and dispersion that is described by the Korteweg-de Vries (KdV) equation. True internal solitary waves do not exist because other factors, such as dissipation, horizontal variability in the stratification, and the earth's rotation, disrupt the nonlinear-dispersion balance. Therefore, although it is often more appropriate to refer to such waves in the ocean as internal "solitary-like" waves, it is common to refer to them simply as internal solitary waves. Despite the approximation, internal solitary waves in the ocean can be described very well by the KdV equation, the solution of which gives a "rank-ordered" train of internal solitary waves because larger-amplitude internal solitary waves propagate faster and hence are ahead of the shorter-amplitude waves in the train. The KdV equation governs the evolution of internal solitary waves in weakly-nonlinear conditions, for example over gentle slopes, and predicts that a wave will undergo a change in polarity, from a wave of depression to a wave of elevation, as it passes a critical point at which the mixed-layer depth is equal to half the water depth. After forming as a result of this gentle shoaling process, internal solitary waves of elevation continue propagating upslope as bores or boluses with similar dynamics to those discussed above.

### Breaker Classifications

Further study of the shoaling process has shown that there is a distinction between the formation of internal solitary waves of elevation due to polarity reversal and the formation of upslope surging boluses. Polarity reversal occurs when the rear faces of solitary waves of depression steepen, since the internal solitary wave trough propagates more slowly than its tail as it moves into shallow water. During this process, a "positive tail" is formed behind the wave. Then, if the steepening time scale is long enough, the tail morphs into a train of solitary waves of elevation. This occurs on gentle slopes, and is referred to a fission breaker (Fig. 4A). Increasing the slope leads to plunging, collapsing, and surging breakers (Aghsaee et al. 2010), as shown in Fig. 4B–D. The fission process is related to the canonical behavior of breaking internal waves at low Iribarren numbers, while the steeper slope breaking mechanisms are associated with noncanonical breaking at higher Iribarren numbers.

Fission breaking is the most common in the ocean because of the relatively gentle slopes $s \leq O(0.01)$ found on the continental shelf and in nearshore regions (hence why canonical breaking is expected in most of the ocean). Perhaps the most comprehensive observation of a shoaling and breaking internal solitary wave is presented by Bourgault et al. (2007), who used a towed echosounder to follow an internal solitary wave of depression through the entire fission process. The small time and spatial scales

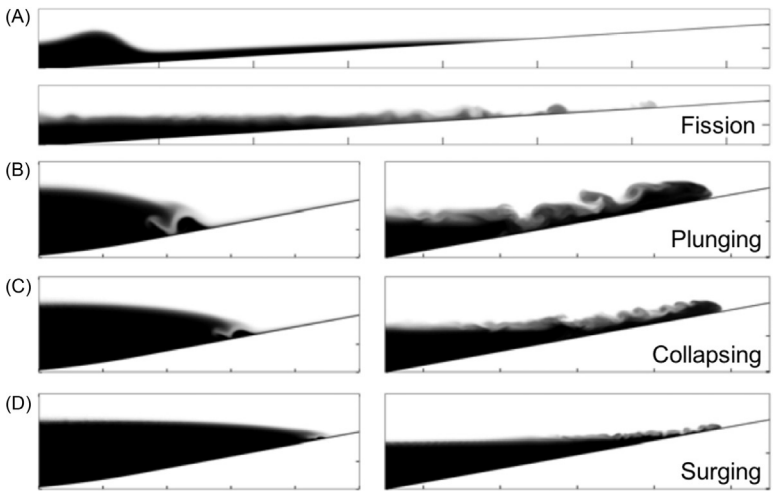


**Fig. 4** Examples of (A) fission, (B) plunging, (C) collapsing, and (D) surging internal solitary wave breakers from the direct numerical simulations of Arthur and Fringer (2014). Each wave is shown at the breaking point and during the upslope progression of dense water that follows.

of internal solitary wave breaking events, as well as their unpredictable nature, makes capturing them in the field quite difficult. For this reason, a substantial amount of internal solitary wave breaking research has made use of idealized experiments in the laboratory and in numerical models.

### Mixing and Mixing Efficiency

The dynamics of each internal solitary wave breaker type determines the resulting amount of mixing during the breaking process (see Fig. 5A). Plunging breakers, which create the most vigorous overturning, lead to the most mixing, followed by fission breakers, which have a longer time scale for mixing over the length of the gentle slope. These are followed by collapsing, then surging breakers. Mixing is generally more sensitive to the wave amplitude, which is proportional to the wave energy, than to the topographic slope, which affects the time scale of the breaking event. Intuitively, for a given topographic slope, larger amplitude waves, which have more incoming energy, have larger total mixing values. For a given wave amplitude, more mixing occurs over gentler slopes due to the increased time scale of the breaking event. The turbulent dissipation of internal solitary wave energy that occurs during breaking follows similar trends (Fig. 5A).

Several internal solitary wave breaking studies have focused on quantifying the mixing efficiency because of its importance in estimating ocean mixing from observed vertical density profiles. In the context of breaking internal waves, the bulk mixing efficiency is often presented as the total amount of mixing that occurs during a breaking event relative to the total irreversible energy loss, which includes both dissipation and mixing. As shown in Fig. 5B, Boegman et al. (2005), using the data of Michallet and Ivey (1999), report bulk mixing efficiency values between roughly 5% and 25%, while Arthur and Fringer (2014) report values between 13% and 21%, depending on the internal Iribarren number. By decreasing the strength of the stratification, Arthur et al. (2017) found bulk mixing efficiency values as high as 31%.

#### *A note on the internal Iribarren number*

Several of the aforementioned studies have presented internal solitary wave breaker classifications and mixing efficiency results as a function of the internal Iribarren number $\xi$. While $\xi$ is an appropriate classifier for internal tides, which have long wavelengths relative to their amplitude, it is important to note its limitations in classifying internal solitary wave breakers, which generally have shorter wavelengths and thus steeper wave slopes $a/\lambda$. In particular, $\xi$ does not necessarily uniquely define internal solitary wave properties, such as breaker type or mixing efficiency, for a given wave and topographic slope (as seen in Fig. 5). It is therefore more appropriate to classify internal solitary wave breaking in terms of a two-dimensional parameter space defined by the topographic slope and the wave steepness. Aghsaee et al. (2010, see Fig. 6 therein) showed that the breaker type (i.e., fission, plunging, collapsing, or surging) can be uniquely classified in this way. However, mixing and mixing efficiency results within this parameter space have not yet been fully explored.

## Mass and Sediment Transport Driven by Internal Wave Breaking

Shoaling and breaking internal waves, including both internal tides and internal solitary waves, are known to cause the transport of ecologically relevant scalars in the coastal ocean, including heat, sediment, nutrients, larvae, plankton, and dissolved oxygen. Along

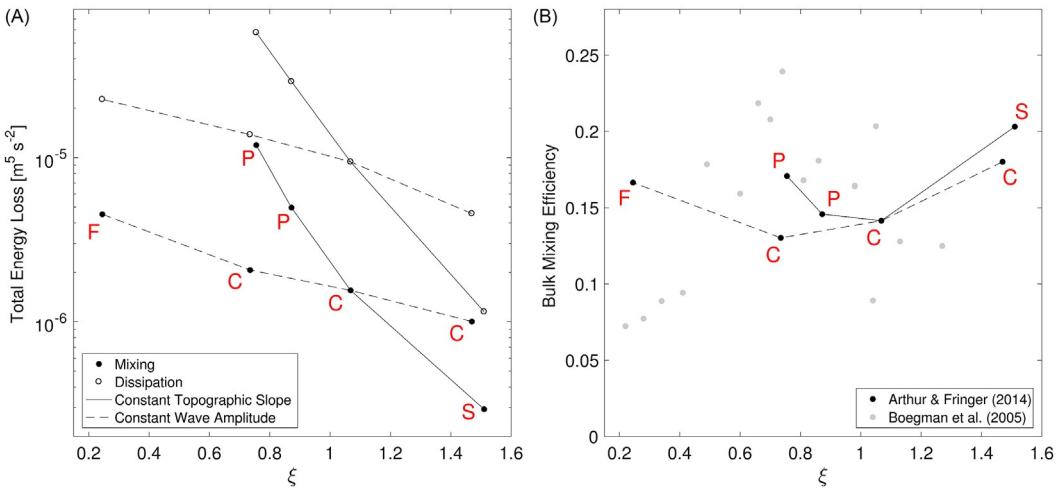


**Fig. 5** (A) Total mixing and dissipation from the internal solitary wave breaking simulations of Arthur and Fringer (2014). (B) The bulk mixing efficiency of internal solitary wave breaking events from Arthur and Fringer (2014) and Boegman et al. (2005). *Red letters* indicate the internal solitary wave breaker classification (F = Fission, P = Plunging, C = Collapsing, S = Surging) for the cases of Arthur and Fringer (2014).

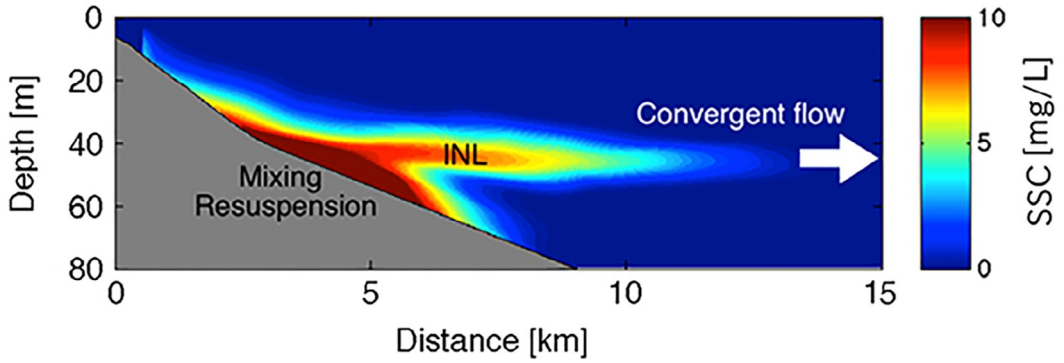


**Fig. 6** Numerical simulation of an intermediate nepheloid layer due to internal wave breaking (Masunaga et al., 2017).

with other transport mechanisms such as surface wave-driven flows, wind-driven flows, and river outflows, breaking internal waves contribute to the high productivity of the coastal ocean relative to open seas. However, breaking internal waves have also been shown to create ecological hazards in the coastal ocean, including the formation of red tides (or intense phytoplankton blooms) at Huntington Beach, CA, United States (Omand et al., 2011) and the development of hypoxic (low dissolved oxygen) events in Monterey Bay, CA, United States (Booth et al., 2012).

Breaking internal waves can drive both offshore and onshore-directed transport in the coastal ocean. Locally intensified mixing on a slope can lead to the development of a horizontal buoyancy gradient that drives an offshore convergent flow, often referred to as a tertiary circulation. Recent numerical experiments show that mixing due to internal tide breaking contributes to the development of convergent flows with velocities reaching 0.05 m $s^{-1}$. Onshore transport has also been observed during the upslope propagation of the bores or boluses created by breaking internal waves. The vortex cores associated with these features sometimes contain "trapped" dense fluid and scalars that can be transported long distances onshore.

Much of the research on breaking internal wave driven transport has focused on sediment, which is often observed in the backscatter signal of acoustic instruments that are used to measure velocity in the ocean (e.g., acoustic Doppler current profilers, or ADCPs). Sediments that are suspended by the bottom shear stress induced by internal wave breaking can be transported offshore by convergent flows or onshore within bores or trapped cores. The offshore transport of sediment associated with both breaking internal tides and internal solitary waves often occurs within a high concentration along the pycnocline known as an intermediate nepheloid layer (Fig. 6). Because sediments in coastal regions contain high concentrations of nutrients and organic material, knowledge of sediment transport is key to understanding ocean ecosystems.

## Summary and Outlook

Breaking internal waves are a fascinating physical phenomenon that play an important role in ocean dynamics. The mixing and transport processes associated with internal wave breaking affect both the ocean energy budget and coastal ecosystem function. While this chapter has summarized the current scientific understanding of breaking internal waves in the coastal ocean, many questions remain open to future research. For example, how much mixing and dissipation do breaking internal waves contribute to the global ocean energy budget relative to other processes? Or, what parameters control sediment resuspension and transport by breaking internal waves? And finally, how can breaking internal waves change, both positively and negatively, the health of coastal ecosystems?

Much of the recent progress in internal wave research has been enabled by technological advancements in ocean instrumentation, new observation techniques, and improved numerical and laboratory approaches. However, the application of these research methods to breaking internal waves has not been fully explored. In the immediate future, scientific understanding of breaking internal waves can be improved by observing the evolution of internal waves as they shoal and break on coastal slopes. Towed instruments, cabled mooring arrays, and autonomous underwater vehicles should be exploited for this purpose. In conjunction with observations, numerical models of breaking internal waves should utilize adaptive mesh refinement or grid nesting to capture the evolution of internal waves from the offshore to the nearshore, focusing computational resources on fine-scale breaking processes.

## Acknowledgments

A portion of this work was prepared by LLNL under Contract DE-AC52-07NA27344. OBF acknowledges the support of ONR Grants N00014-16-1-2256 and N00014-15-1-2287.

## References

Aghsaee P, Boegman L, and Lamb KG (2010) Breaking of shoaling internal solitary waves. *Journal of Fluid Mechanics* 659: 289–317.

Arthur RS and Fringer OB (2014) The dynamics of breaking internal solitary waves on slopes. *Journal of Fluid Mechanics* 761: 360–398.

Arthur RS, Koseff JR, and Fringer OB (2017) Local versus volume-integrated turbulence and mixing in breaking internal waves on slopes. *Journal of Fluid Mechanics* 815: 169–198.

Boegman L, Ivey GN, and Imberger J (2005) The degeneration of internal waves in lakes with sloping topography. *Limnology and Oceanography* 50(5): 1620–1637.

Booth JAT, McPhee-Shaw EE, Chua P, Kingsley E, Denny M, Phillips R, Bograd SJ, Zeidberg LD, and Gilly WF (2012) Natural intrusions of hypoxic, low pH water into nearshore marine environments on the California coast. *Continental Shelf Research* 45: 108–115.

Bourgault D, Blokhina MD, Mirshak R, and Kelley DE (2007) Evolution of a shoaling internal solitary wave train. *Geophysical Research Letters* 34(3).

Masunaga E, Fringer OB, Yamazaki H, and Amakasu K (2016) Strong turbulent mixing induced by internal bores interacting with internal tide-driven vertically-sheared flow. *Geophysical Research Letters*. https://doi.org/10.1002/2016GL067812.

Masunaga E, Arthur RS, Fringer OB, and Yamazaki H (2017) Sediment resuspension and the generation of intermediate nepheloid layers by shoaling internal bores. *Journal of Marine Systems* 170: 31–41.

Michallet H and Ivey GN (1999) Experiments on mixing due to internal solitary waves breaking on uniform slopes. *Journal of Geophysical Research: Oceans* 104(C6): 13467–13477.

Omand MM, Leichter JJ, Franks PJ, Guza RT, Lucas AJ, and Feddersen F (2011) Physical and biological processes underlying the sudden surface appearance of a red tide in the nearshore. *Limnology and Oceanography* 56(3): 787–801.

Sasmal K, Masunaga E, Webb A, Fringer OB, Gross ES, Rayson MD, and Yamazaki H (2018) A three-dimensional numerical study of river plume mixing processes in Otsuchi Bay, Japan. *Journal of Oceanography* 74(2): 169–186.

## Further Reading

Arthur RS and Fringer OB (2016) Transport by breaking internal gravity waves on slopes. *Journal of Fluid Mechanics* 789: 93–126.

Walter RK, Woodson CB, Arthur RS, Fringer OB, and Monismith SG (2012) Nearshore internal bores and turbulent mixing in southern Monterey Bay. *Journal of Geophysical Research, Oceans* 117(C7): C07017.